

## Recent Changes in Average Recurrence Interval Precipitation Extremes in the Mid-Atlantic United States

ARTHUR T. DEGAETANO<sup>a</sup> AND HARRISON TRAN<sup>a</sup>

<sup>a</sup> *Northeast Regional Climate Center, Cornell University, Ithaca, New York*

(Manuscript received 2 July 2021, in final form 20 December 2021)

**ABSTRACT:** Increases in the frequency of extreme rainfall occurrence have emerged as one of the more consistent climate trends in recent decades, particularly in the eastern United States. Such changes challenge the veracity of the conventional assumption of stationarity that has been applied in the published extreme rainfall analyses that are the foundation for engineering design assessments and resiliency planning. Using partial-duration series with varying record lengths, temporal changes in daily and hourly rainfall extremes corresponding to average annual recurrence probabilities ranging from 50% (i.e., the 2-yr storm) to 1% (i.e., the 100-yr storm) are evaluated. From 2000 through 2019, extreme rainfall amounts across a range of durations and recurrence probabilities have increased at 75% of the long-term precipitation observation stations in the mid-Atlantic region. At approximately one-quarter of the stations, increases in extreme rainfall have exceeded 5% from 2000 through 2019, with some stations experiencing increases in excess of 10% for both daily and hourly durations. At over 40% of the stations, the rainfall extremes based on the 1950–99 partial-duration series show a significant ( $p > 0.90$ ) change in the 100-yr ARI relative to the 1950–2019 period. Collectively, the results indicate that, given recent trends in extreme rainfall, routine updates of extreme rainfall analyses are warranted on 20-yr intervals.

**SIGNIFICANCE STATEMENT:** Engineering design standards for drainage systems, dams, and other infrastructure rely on analyses of precipitation extremes. Often such structures are designed on the basis of the probability of exceeding a specified rainfall rate in a given year. The frequency of extreme rainfall events has increased in the mid-Atlantic region of the United States in recent decades, leading us to evaluate how these changes have affected these exceedance probabilities. From 2000 through 2019, there has been a consistent increase of generally 2.5%–5.0% in design rainfall amounts. The increase is similar across a range of rainfall durations from 1 h to 20 days and also annual exceedance probabilities ranging from 50% to 1% (i.e., from the “2-yr storm” to the “100-yr storm”). The work highlights the need to routinely update the climatological extreme-value analyses used in engineering design, with the results suggesting that a 20-yr cycle might be an appropriate update frequency.

**KEYWORDS:** Extreme events; Precipitation; Trends; Climate services

### 1. Introduction

Numerous authors (Groisman et al. 2012; Kunkel et al. 2013; Walsh et al. 2014) have identified recent trends in extreme rainfall (e.g., daily events greater than the 99th percentile) in the eastern United States. In addition, parts of the region have also experienced a documented increase in flooding and rainfall events that are conducive to flooding, especially in urban environments (Collins 2009; DeGaetano 2009; Armstrong et al. 2014; Peterson et al. 2013; Georgakakos et al. 2014). Although similar trends have been documented in other parts of the United States (Groisman et al. 2012; Cooley and Chang 2017; Brown et al. 2020) and the globe (Groisman et al. 2005; Fischer and Knutti 2016; Lenderink et al. 2011), the magnitudes of the trends in the mid-Atlantic region of the United States are particularly strong.

Increasing average temperatures lead to both increases in atmospheric water vapor and the frequency of convective storm events (Coumou and Rahmstorf 2012) that have been implicated as physical reasons for these changes. In addition, changes in frequency, intensity, and tracks of tropical and extratropical cyclones contribute to trends in extreme precipitation (e.g., Shepherd et al. 2007; Lau et al. 2008; Prein and Mearns 2021). In some cases, linkages to certain atmospheric circulation patterns have been posed as influencing changes in precipitation extremes (e.g., Kenyon and Hegerl 2010). Nevertheless, climate model simulations suggest that extreme precipitation events will continue to increase through the twenty-first century (e.g., Donat et al. 2016; Ning et al. 2015; Sun et al. 2016).

A practical consequence of these increases in extreme precipitation frequency (DeGaetano 2009; Groisman 1992; Heineman 2012; Kunkel et al. 1999; Kunkel 2003) is that the assumption of a stationary climate record compromises the specifications used to design infrastructure. For example, DeGaetano (2009) reports that rainfall amounts once considered to be 1-in-100-yr events, as based on the data record available from 1950 to 1978, occur as often as once every 67 years as based on data observed across the Northeast from 1978 to 2008 and with even greater frequency through the twenty-first century (e.g., DeGaetano and Castellano 2017).

© Supplemental information related to this paper is available at the Journals Online website: <https://doi.org/10.1175/JAMC-D-21-0129.s1>.

Corresponding author: Art DeGaetano, atd2@cornell.edu

Despite these established trends in extreme rainfall, recent flooding disasters and the range of climate-related risks and vulnerabilities associated with extreme rainfall, design standards and regulations in much of the region are currently based on climate data that has not been analyzed since 2000 (Bonnin et al. 2006). Infrastructure design has long relied on statistical extreme-value analysis (Yarnell 1935), in which an extreme-value function is fitted to a relevant observed time series, resulting in a “design storm.” For these design storms, the  $n$  highest values from the observed precipitation record are typically extracted and analyzed to yield the probability of exceeding a specific rainfall amount. These probabilities are often referred to as average recurrence intervals (ARI).

This, of course, assumes that the historical probabilities apply to future conditions. However, given the many studies documenting observed and projected increases in extreme precipitation frequency, this assumption may no longer be valid, depending on the partial-duration series period of record, specific station, return period and accumulation duration (e.g., Cheng and AghaKouchak 2014a; Myhre et al. 2019). To accommodate trends in precipitation, some extreme-value analyses incorporate nonstationarity in the underlying extreme-value function (Katz 2010; Cheng et al. 2014b).

Given the observed trends in extreme rainfall, particularly across the mid-Atlantic United States, it is unclear how the inclusion of 19 additional years of rainfall data have affected the rainfall extremes published in 2000. Since several locations have experienced record rainfall events since 2000, or at least rainfall events comparable to the highest in the pre-2000 record, it is likely that the values published in NOAA Atlas 14 (Bonnin et al. 2006) underestimate the rainfall extremes that factor in the more recent years of data. This study quantifies the changes in extreme rainfall recurrence amounts since 2000 across the region. In section 2, the underlying data are described, which include precipitation accumulation at both daily and hourly time scales. The methods used to analyze these datasets and determine the statistical significance of the observed differences are outlined in section 3. The results are summarized in section 4, including a discussion of how recent extreme rainfall events and length of the precipitation record affect ARI estimates. In the concluding section, attention is paid to how the results might be applied in scheduling routine updates to published extreme rainfall statistics.

## 2. Data

Daily Cooperative Observing Network stations within the area extending from  $46.0^{\circ}$  to  $36.0^{\circ}$ N and from  $84.0^{\circ}$  to  $71.0^{\circ}$ W were identified. From these locations, a set of 480 base sites was retained on the basis of the following criteria: 1) inclusion in NOAA Atlas 14, volume 2 or volume 10 (Bonnin et al. 2006; Perica et al. 2019), 2) a data record that extends from at least 1950 through 2019, and 3) less than 5% of daily precipitation missing. Similarly, a larger set of regional stations was retained that included the base stations and additional sites having at least 20 years of record after 1980. For all sites, daily rainfall observations and data quality flags were extracted from the

Applied Climate Information System (ACIS) and reflect the values in the Global Historical Climatology Network Daily (GHCN-D; Menne et al. 2012) on 13 January 2021.

Similar criteria were used to select hourly observing stations. These sites were extracted from one of three databases: 1) NOAA National Centers for Environmental Information (NCEI) COOP-Hourly Precipitation Data (HPD), version 2 (Wuertz et al. 2018), for stations with available records after 2014; 2) NCEI’s Hourly Precipitation Dataset (HPD), known historically as DSI-3240 (<https://www.ncdc.noaa.gov/metadata/geoportal/rest/metadata/item/gov.noaa.ncdc:C00313/html#>) for stations with records ending prior to 2014; and 3) NCEI Surface Data Hourly Global (DS3505) for National Weather Service Automated Surface Observing System stations. A total of 92 base hourly stations were available within the study region.

Using the daily rainfall data, partial-duration rainfall series (PDS) were formulated for the base and regional stations. Similar PDS were obtained using hourly data. Separate PDS were developed for 1-, 2-, 3-, 7-, 10-, and 20-day and 1-, 2-, 3-, 6-, 12-, 24-, and 48-h precipitation accumulations. Daily precipitation values flagged as “accumulated” were retained if the accumulation period was less than or equal to the indicated duration. For example, a value that represented a 2-day accumulation was excluded from the 1-day PDS but was included as part of the 2-or-greater-day PDS. When multiple PDS members occurred within a 14-day window, the smaller value was excluded from the PDS, to satisfy the requirement that PDS members were independent. This time interval was selected to approximate the time scale of unique synoptic weather patterns. The temporal independence for hourly data was a function of duration, ranging from 24 h for durations from  $\leq 3$  to 336 h (14 days) for durations  $\geq 24$  h. Events in the 6- and 12-h-duration PDS were required to be separated by more than 48 and 168 h (7 days), respectively.

For each station, an array of 29 PDS was generated such that the shortest PDS included data from 1950 to 1990 and the longest was based on data from 1950 to 2019. In each case, the PDS contained  $n$  values, where  $n$  was defined as the total number of nonmissing precipitation values divided by the total number of days or hours in the relevant period of record rounded to an integer. The use of these standard time periods was necessary to allow comparisons among stations. Using variable record lengths, including the inclusion of data prior to 1950, would preclude such comparisons. The use of 50–70-yr records maximizes the number of stations available for analysis and limits the influence of data from earlier years that may not be representative of recent climate conditions while assuring an adequate sample size for extreme-value analysis (DeGaetano and Castellano 2018). Records of this length also mitigate the influence of interdecadal variations in rainfall, which may influence shorter time series (Yu et al. 2016).

## 3. Methods

### a. Computation of recurrence interval rainfall amounts

Using the array of 29 PDS at each station, rainfall amounts corresponding to recurrence probabilities of 50%, 20%, 10%,

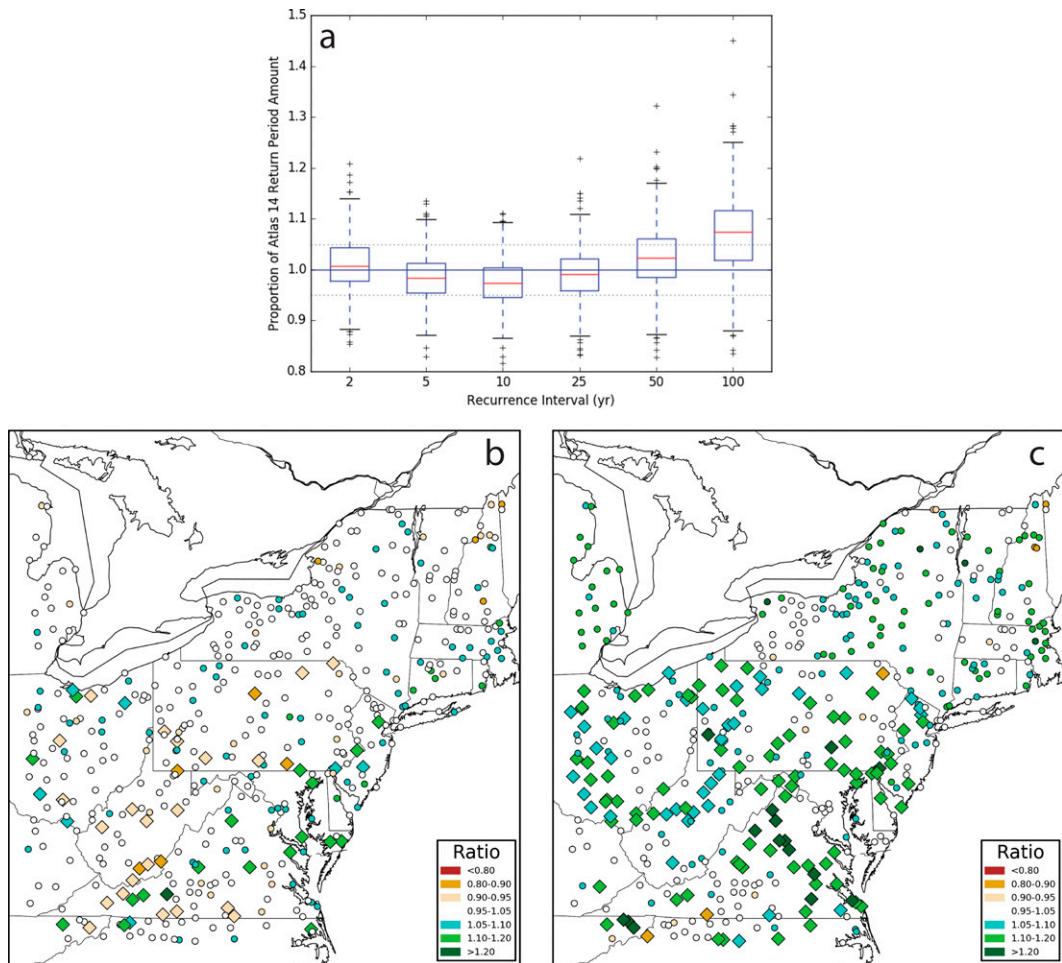


FIG. 1. Differences between 1-day (converted to 24 h) Atlas 14 and project-computed recurrence interval rainfall amounts. (a) Boxplots show differences for all recurrence intervals across all stations in the study domain in (b), with the horizontal dotted lines denoting a  $\pm 5\%$  difference between the values. Station-specific differences are shown for the (b) 2- and (c) 100-yr recurrence interval amounts. The circular station markers indicate computed values that fall within the published Atlas 14 confidence interval, with values falling outside the confidence interval denoted by diamonds.

4%, 2%, and 1% (i.e., 2-, 5-, 10-, 25-, 50-, and 100-yr storms) were computed by simulating the methodology used in NOAA Atlas 14 (Bonnin et al. 2006; Perica et al. 2019). First, the Python L-moments package (<https://pypi.org/project/lmoments/>) was used to fit the generalized extreme value (GEV) distribution to each station's 29 PDS using the methods of Hosking (1990). Other theoretical extreme-value distributions exist, but the GEV has been used extensively in prior extreme rainfall analyses (e.g., Papalexiou and Koutsoyiannis 2013). Given the L-moments estimates for the GEV parameters, the L-moments library method was used to obtain the specified quantiles of the GEV distribution.

The regional L-moments procedure used in NOAA Atlas 14, volume 10 (Perica et al. 2019), was adapted. Although most sites lie outside the region covered by this atlas, the difference in methodology employed to develop regions in the later atlas was an improvement over the earlier implementation. A

maximum of 20 neighboring stations, identified from the previous set of regional stations, formed a region around each base station. Sample L-moments were obtained for each regional station using the L-moments library "samlmu" routine, and a weighted average of the higher-order moments was computed on the basis of the length of each station's PDS. These weighted averages along with the base station's location parameter were then used to obtain GEV parameters and quantiles.

Although this did not exactly replicate the Atlas 14 methodology, the differences between the resulting ARI rainfall amounts and those given by Atlas 14 were generally small, with most values falling within the published Atlas 14 confidence intervals (Figs. 1 and 2). For the daily return periods, approximately 40% of the stations' 2-yr ARI amounts were within  $\pm 2.5\%$  of the corresponding Atlas 14 value, with over 75% within  $\pm 5\%$  of the published value. For the 5- and 10-yr ARI, values tended to be lower than the Atlas 14 values, but

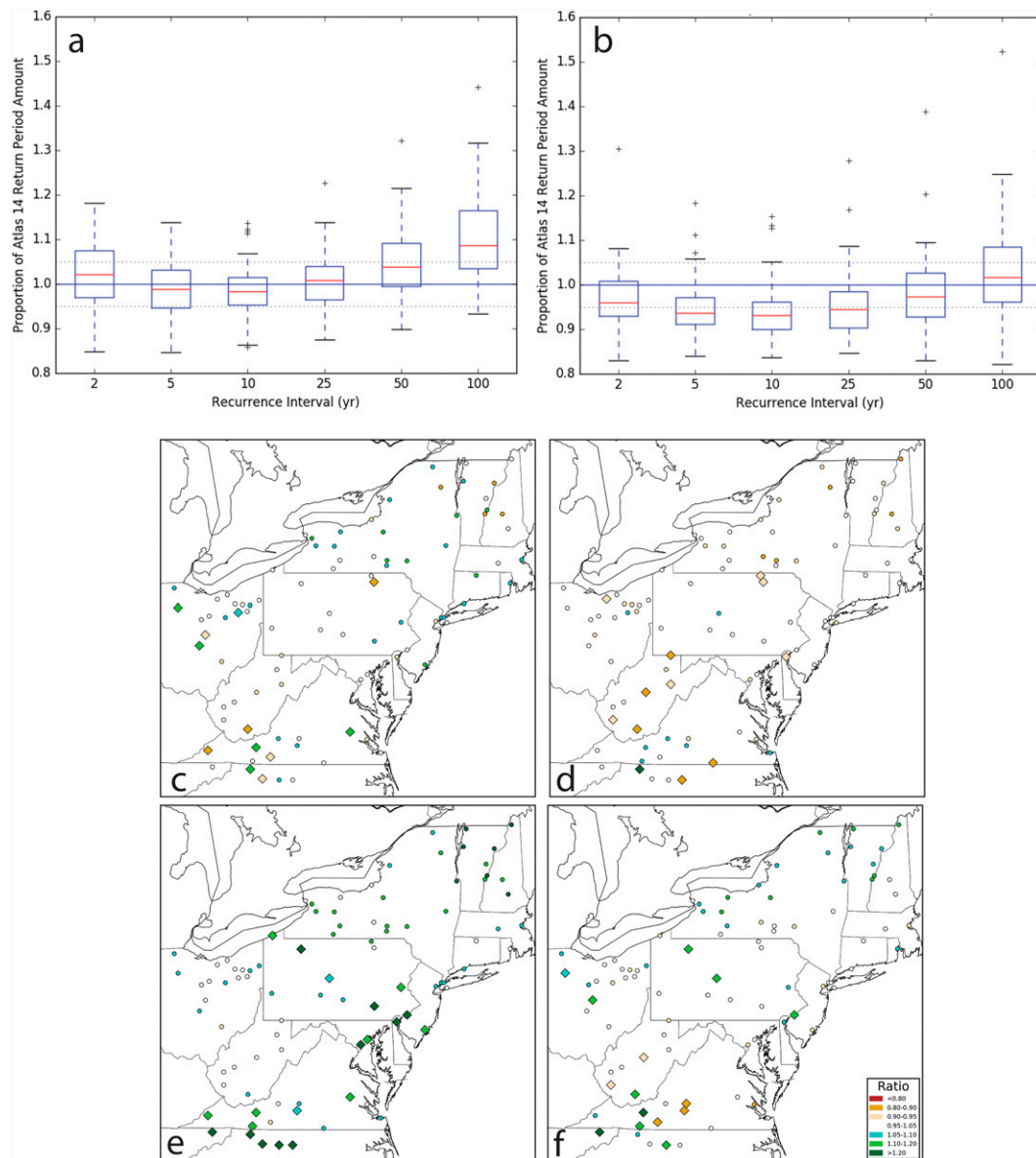


FIG. 2. Differences between (a) 1-h (converted to 60 min) and (b) 24-h Atlas 14 and project-computed recurrence interval rainfall amounts. Boxplots show differences for all recurrence intervals across all stations in the study domain with the horizontal dotted lines denoting a  $\pm 5\%$  difference between the values. Station-specific differences are shown for the (c) 2-yr 1-h, (d) 2-yr 24-h, (e) 100-yr 1-h, and (f) 100-yr 24-h recurrence interval amounts. The circular station markers indicate computed values that fall within the published Atlas 14 confidence interval, with values falling outside the confidence interval denoted by diamonds.

for longer ARI most of the differences became positive. For the 50-yr ARI, the median difference between the two computation methods was  $+2.5\%$ , whereas for the 100-yr storm approximately one-half of the stations' ARI amounts were over  $7.5\%$  higher than the published Atlas 14 values.

Although there is not a clear geographic bias to the differences, the 100-yr ARI values computed for stations in New York and New England always fall within the Atlas 14 confidence intervals (Figs. 1b,c). In the southern part of the region, even

though the differences are of the same magnitude as those for stations in the northern states, the values tend to fall outside the Atlas 14 confidence bounds more frequently. This results from the changes in the Atlas 14 methodology used to regionalize stations and compute confidence intervals. The methodology used in the earlier volume 2 consistently resulted in narrower confidence interval widths relative to the newer procedure.

Differences in the lengths of the period of record used in Atlas 14, in comparison with the fixed 1950 starting point

record used in this study, contribute to the overestimation of 100-yr ARI amounts relative to 2-yr values. For example, a >20% difference occurred at Wilmington Porter Reservoir in Delaware (Fig. 1c) for which the Atlas 14 rainfall record begins in 1933. The PDS values that occurred prior to 1950 are systematically smaller, with only 2 of the potential 17 PDS years (12%) recording rainfall > 9.27 cm (the 1-day 5-yr storm), whereas, in the period from 1950 to 2000, 17 of the 51 years (33%) record rainfall exceeding this value. Thus, the prevalence of positive differences reflects the tendency for extreme rainfall to increase with time (e.g., DeGaetano 2009) and also the potential for the longer PDS length in Atlas 14 to temper the extremes. Since subsequent analyses were based on differences in recurrence interval rainfall amounts between the longer (1950–2019) and shorter (1950–2000) PDS periods, it was important to adapt a consistent methodology and reference period through time.

The Atlas 14 differences at the subset of stations with hourly data are similar (Fig. 2). Like the daily stations, the differences for the 1- and 24-h amounts display a similar pattern with recurrence interval. In all three cases (daily, 1 h, and 24 h), the simulated procedure underestimates the Atlas 14 10-yr recurrence interval values at most of the stations. The 2-yr ARIs exhibit a similar number of over and underestimates, and the 100-yr ARI amounts are predominately overestimated, especially for the hourly duration (Fig. 2a). Regardless of ARI, the hourly durations are more frequently overestimated relative to the 24-h durations. Collectively, however, like the daily stations, the computed values that are typically within  $\pm 5\%$  of the Atlas 14 value. Also, like the daily stations, there is not a strong geographic pattern to the differences (Figs. 2c–f). Across New York and New England where the Atlas 14 confidence intervals are wider, all the simulated values fall within the Atlas 14 confidence intervals.

#### b. Post-2000 rainfall extreme differences

Given the ARI rainfall amounts for each duration, a percent difference was computed such that

$$\Delta P_{\text{end}} = P(d,r)_{\text{end}}/P(d,r)_{\text{base}},$$

where  $P$  is the precipitation amount corresponding to duration  $d$  and ARI  $r$ . The subscripts “end” and “base” represent the ending years of the two PDS being compared. Although different base years can be used, hereinafter base = 2000. When the end value is 2019,  $\Delta P_{2019}$  compares the ARI using the 1950–2019 PDS with that corresponding to the 1950–2000 PDS used to simulate the Atlas 14, volume 2, record.

The significance of  $\Delta P_{2019}$  was assessed using a resampling analysis. For recurrence interval amounts computed using nonregional L-moments, the GEV parameters fit to the base station’s 1950–2019 PDS were used to randomly generate 1000 PDS using the random variates method in the `scipy.stats.genextreme` library (<https://docs.scipy.org/doc/scipy/reference/generated/scipy.stats.genextreme.html>). For each random (unsorted) PDS, the L-moments procedure was used to fit new GEV parameters using all 70 values in the randomly generated PDS and a second set of GEV parameters based on

only the first 50 of the random PDS values. This was intended to simulate the difference between the current (through 2019) PDS available at a station and that available in 2000. Quantiles were computed from these two GEV distributions and differenced, giving a set of 1000 random  $\Delta P_{2019}$  values from which the one-tailed probability of obtaining the observed  $\Delta P_{2019}$  value was determined.

Two similar procedures were used to obtain randomized  $\Delta P_{2019}$  distributions for the regional L-moments results. In both cases, the GEV parameters obtained from the regional L-moments analysis of the observed PDS (as opposed to those obtained solely for the base station) were used to generate the 1000 random PDS. In the first method, the original weighted regional L-moments were used to obtain new GEV parameters from the randomized PDS that were ultimately used to construct the randomized  $\Delta P_{2019}$  distribution. Thus, while 1000 randomized PDS were generated, only the L-moments location parameter varied in each simulation.

In the second method, random PDS were also generated for each of the regional stations allowing different regionally weighted higher-order L-moments parameters to be used in each random simulation. There are trade-offs to each method. The first likely underestimates the variation of the random  $\Delta P_{2019}$  distribution. The second does not account for any potential autocorrelation in the neighboring PDS as each is generated independently. Nonetheless there was not a systematic difference in the  $\Delta P_{2019}$  probabilities generated by one approach as compared with the other.

## 4. Results

Figure 3 shows  $\Delta P_{2019}$  daily duration boxplots for 2- and 100-yr recurrence intervals. There has been a general increase in extreme rainfall in the 1950–2019 period relative to 1950–2000 as indicated by the medians of all of the boxplots exceeding  $\Delta P_{2019} = 1.00$ . The height of each boxplot represents the variation in  $\Delta P_{2019}$  across the 480 stations shown in Fig. 1. There is little difference in  $\Delta P_{2019}$  relative to ARI or duration (Fig. 3). This is also true for the ARI intervals not shown (Fig. S1 in the online supplemental material). Except for the 100- and 50-yr ARI, 75% of the stations have experienced an increase in extreme precipitation amounts since the publication of Atlas 14 regardless of duration. In general, the median increase is near 2.5%, with about one-quarter of the stations experiencing an increase of between 2.5% and 5%.

These increases occur regardless of whether the ARI precipitation amounts are computed using regional L-moments, which incorporate higher-order moments from up to 20 surrounding stations, or when all moments are based only on PDS from each station individually (Fig. 3). At most stations, the  $\Delta P_{2019}$  values are similar, with increases generally between 0% and 5% for the 2-yr ARI and slightly greater increases indicated for the 100-yr ARI. The most pronounced difference when using the single-station fits is the increase in the number of outliers in the 100-yr ARI  $\Delta P_{2019}$  values, with increases as large as 80% noted for some sites (not visible on truncated y axis) and decreases of 20% occurring for 1- and

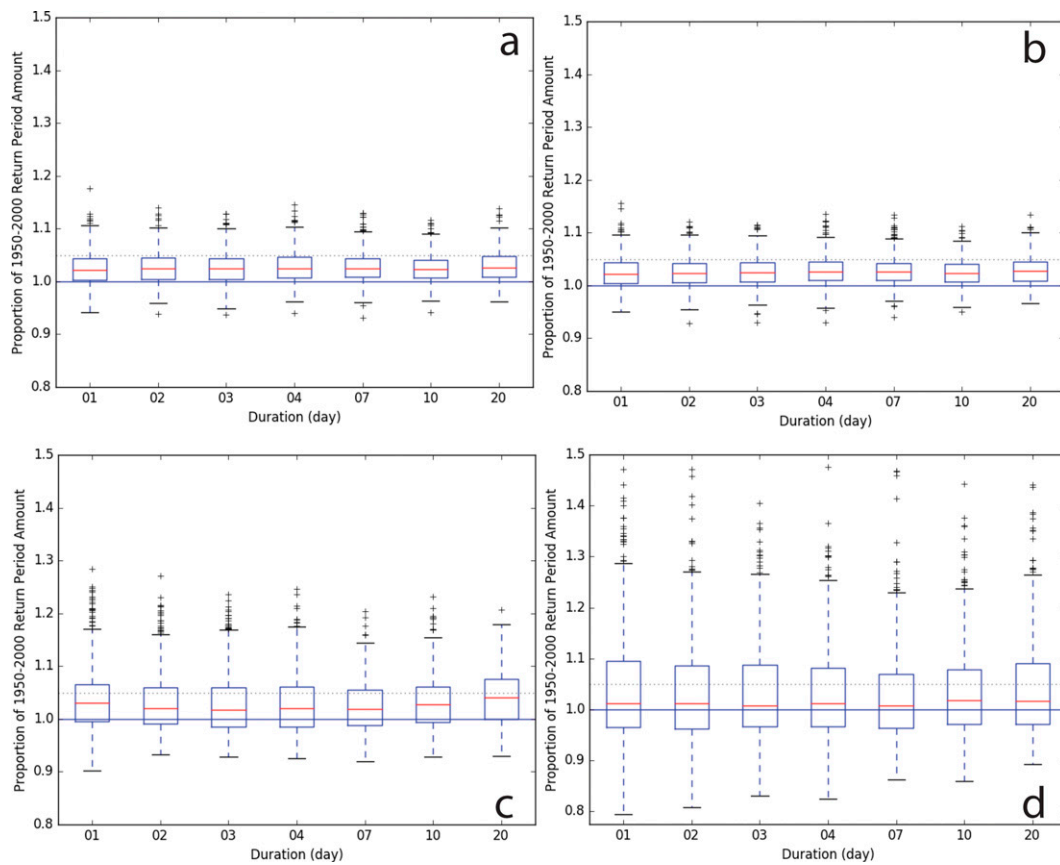


FIG. 3. Boxplots showing the ratios of daily (a), (b) 2- and (c), (d) 100-yr ARI precipitation amounts computed using the 1950–2019 PDS to those based on a 1950–2000 PDS. (left) ARIs are computed using regional L-moments, and (right) values are based on a single-station L-moments fit.

2-day duration events (Fig. 3). Although in the majority of cases the two approaches show similar changes, the regional approach is preferred. It dampens the influence that individual events may introduce in the higher moments, while still accounting for any changes in the fit distributions' location parameter that have occurred in the recent 20-yr period. This is supported by, for example, DeGaetano (2009) and Cheng and AghaKouchak (2014a), who show recent observed changes in precipitation have generally not resulted from significant changes in the higher moments.

The  $\Delta P_{2019}$  boxplots for hourly durations are analogous to those for daily durations (Fig. 4, along with Fig. S2 in the online supplemental material). Regardless of ARI or hourly duration, the median  $\Delta P_{2019}$  values are always  $> 1.0$  and, like the daily values, except for the longest ARI, nearly 75% of the stations have experienced an increase in hourly extreme rainfall since 2000 in the regional analysis. Collectively, the median increase is near 2.5%, with about one-quarter of the stations experiencing an increase of between 2.5% and 5%. Both the regional and single-station L-moments approaches yield similar results, with the exception of more variability for the 100-yr ARI adjustments that is especially due to several large outlier adjustments.

There is not a strong spatial pattern in the  $\Delta P_{2019}$  values for 1-, 7-, or 20-day durations, particularly for the 2-yr ARI (Fig. 5). The prevalence of  $\Delta P_{2019}$  values exceeding 1.0 is readily apparent in Fig. 5, with these values distributed evenly across the region. Likewise, the highest  $\Delta P_{2019}$  values occur across the region as do the stations for which  $\Delta P_{2019}$  is  $< 1$ . For the 100-yr ARI, the spatial patterns of  $\Delta P_{2019}$  are also indistinct. The one exception is for the 7-day duration, where stations exhibiting  $\Delta P_{2019}$  of  $< 1$  have a tendency to be located in the western part of the region from New York southward through Ohio, western Virginia, and West Virginia. This pattern is also prevalent for the 20-day duration, with nearly all stations in New England and along the Atlantic coast showing  $\Delta P_{2019}$  values of  $> 1$ . For hourly durations, a consistent spatial pattern in  $\Delta P_{2019}$  is not readily apparent (Fig. 6).

Figures 7 and 8 illustrate several  $\Delta P_{\text{end}}$  time series. In all cases, the  $\Delta P_{\text{end}}$  corresponding to the year 2000 (i.e.,  $\Delta P_{2000}$ ) is 1.00 by definition. Values greater than 1.00 indicate an increase in rainfall intensity for a particular recurrence interval as data beyond (or before) 2000 are considered. At Philadelphia, Pennsylvania (Fig. 7), there is little difference between the  $\Delta P_{\text{end}}$  values computed using regional versus single station L-moments for the 100-yr ARI based on the hourly

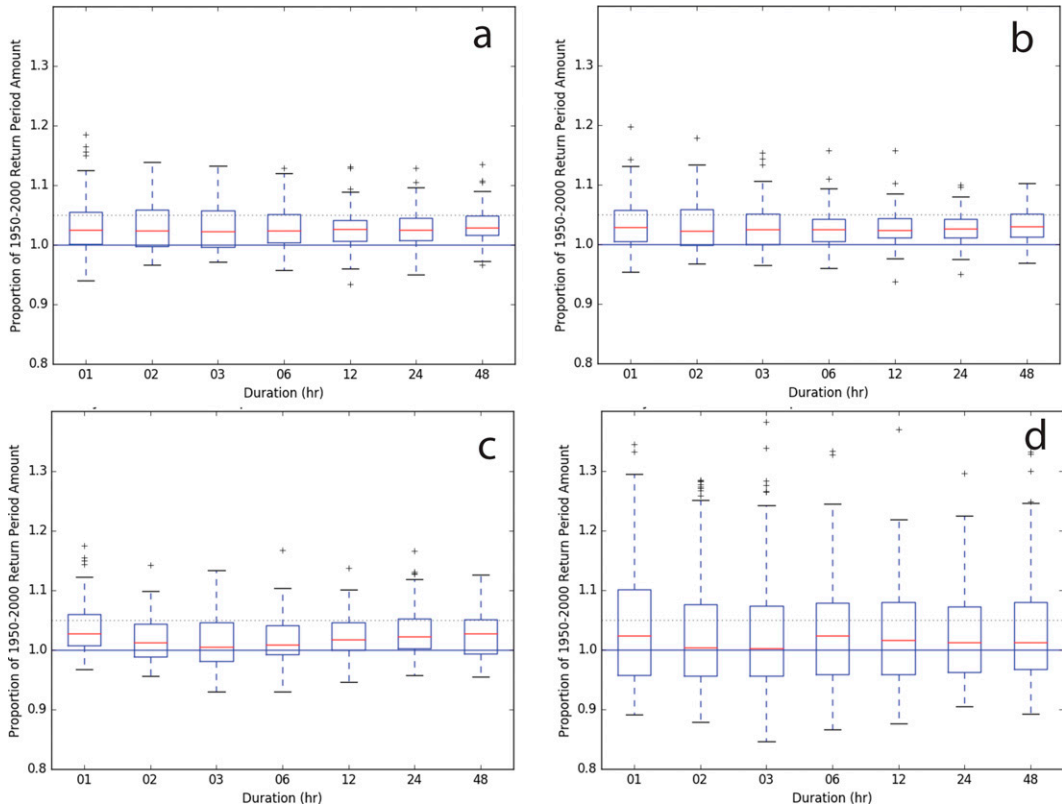


FIG. 4. As in Fig. 3, but for hourly durations.

or daily data record. For the 2-yr ARI, particularly for the 24-h and 1-day durations, the values are also similar with the regional  $\Delta P_{\text{end}}$  values increasing at a slightly faster rate than the single station values, particularly after 2012 when three successive rainfall events became the largest values in the PDS series. The difference in the regional and single-station  $\Delta P_{\text{end}}$  values is more pronounced for the 1-h and 7-day durations.

Figures 7c and 7d also show how  $\Delta P_{\text{end}}$  is affected by the starting date of the PDS. Although  $\Delta P_{\text{end}}$  increases in the post-2000 period when the full 1900–2019 record is used, its change is moderated relative to that based on a 1950 starting date. This is not a consistent response among stations with records that start prior 1950, as it is influenced by the magnitude of the individual rainfall events included in the PDS from the pre-1950 period. At Philadelphia, the 31 largest 24-hourly rainfall events in the full 120-yr PDS occur in the post-1950 period. Furthermore, only 9 of the 120 PDS values occurred prior to 1950; hence the full-record ARI amounts fall below those based on the 1950–2019 values.

Time series of  $\Delta P_{\text{end}}$  are compared for two sets of adjacent stations in Fig. 8, one along the Massachusetts–New Hampshire border and the other set in western Pennsylvania. These station pairs were selected such that at one station the daily  $\Delta P_{2019}$  value exceeds 1.00, indicating that the extreme rainfall has increased since 2000, while the other station is characterized by  $\Delta P_{2019} < 1.00$ . At Middleton, Massachusetts (Fig. 8a),

the 100-yr ARI daily  $\Delta P_{2019}$  is  $< 0.95$ , whereas at Concord, New Hampshire (Fig. 8b), this  $\Delta P_{2019}$  exceeds 1.10. These differences arise due to the magnitudes of the PDS events that were added in the post-2000 period. At Concord, new PDS maxima occurred in 2005 and 2006. This combination of events caused the new 100-yr ARI amount to increase by more than 10%. Two additional years experience a daily rainfall total that exceeds the 90th percentile of the PDS. These result in smaller increases in the 100-yr ARI amount ( $< 1\%$ ). Years in which the PDS additions fall between the 50th and 90th percentile of the PDS result in constant or slowing declining ARI amounts.

At Middleton (Fig. 8a), the post-2000 period is mainly characterized by new PDS entries that fall below the median. This results in a fairly steady decline in the 100-yr ARI precipitation as the record length expands without the occurrence of new extremes. The only increase noted in the post-2000 period is associated with the  $>90$ th percentile event in 2006. While both stations experienced relatively large daily rainfalls in 2005 and 2006, the more extreme magnitude of both events at Concord, relative to the other PDS members results in the overall increase in 100-yr ARI precipitation.

At Indiana 3 SE and Schenley Lock 5 in Pennsylvania, the behavior of the  $\Delta P_{\text{end}}$  series for 2-yr ARI is similar (not shown). Mainly submedian PDS additions and no new PDS maxima lead to a steady decline in 100-yr ARI precipitation as the record length increases at Indiana 3 SE (Fig. 8c),

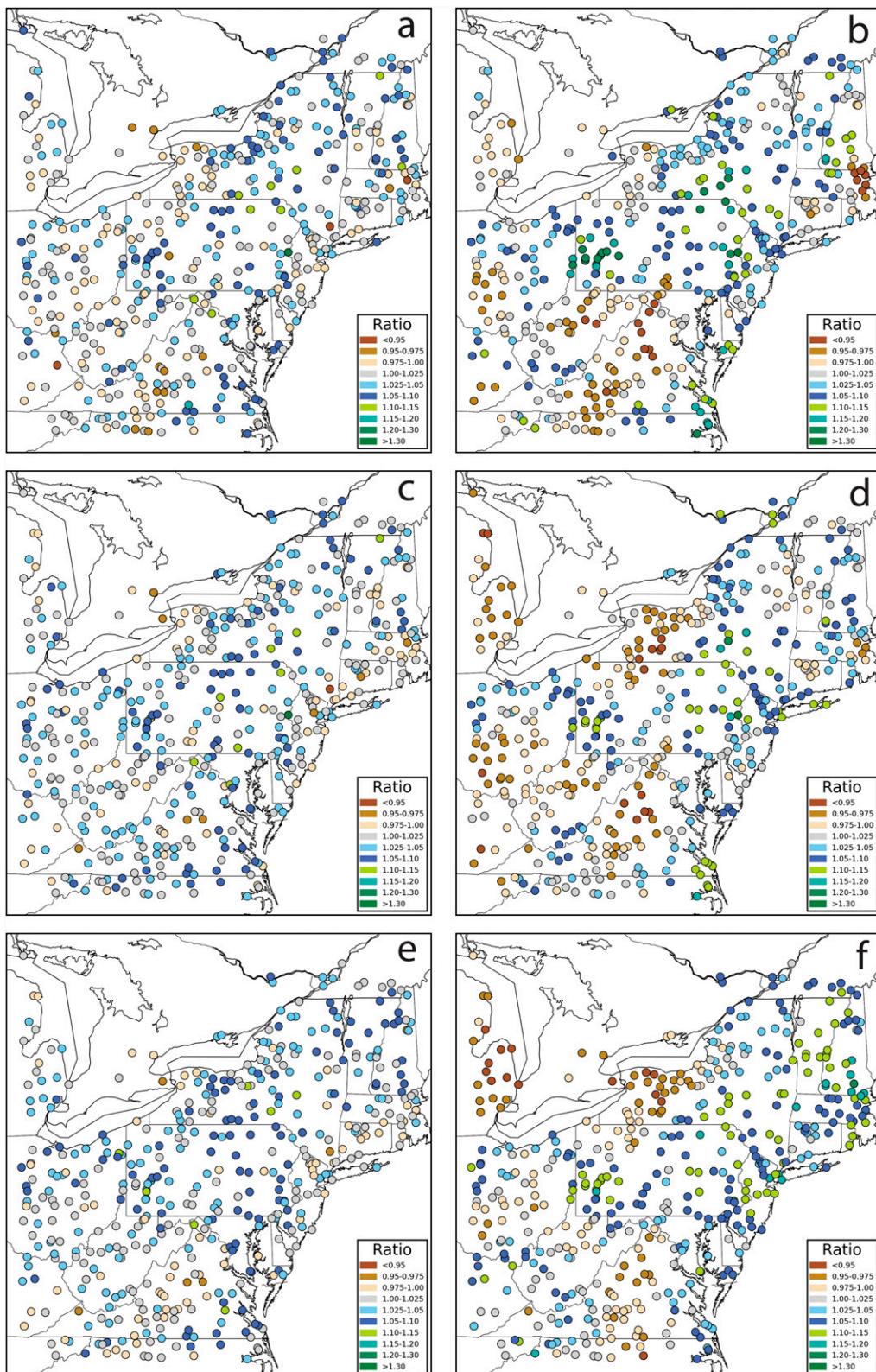


FIG. 5. Station-specific  $\Delta P_{2019}$  ratios for (a) 1-day 2-yr, (b) 1-day 100-yr, (c) 7-day 2-yr, (d) 7-day 100-yr, (e) 20-day 2-yr, and (f) 20-day 100-yr ARI rainfall amounts.

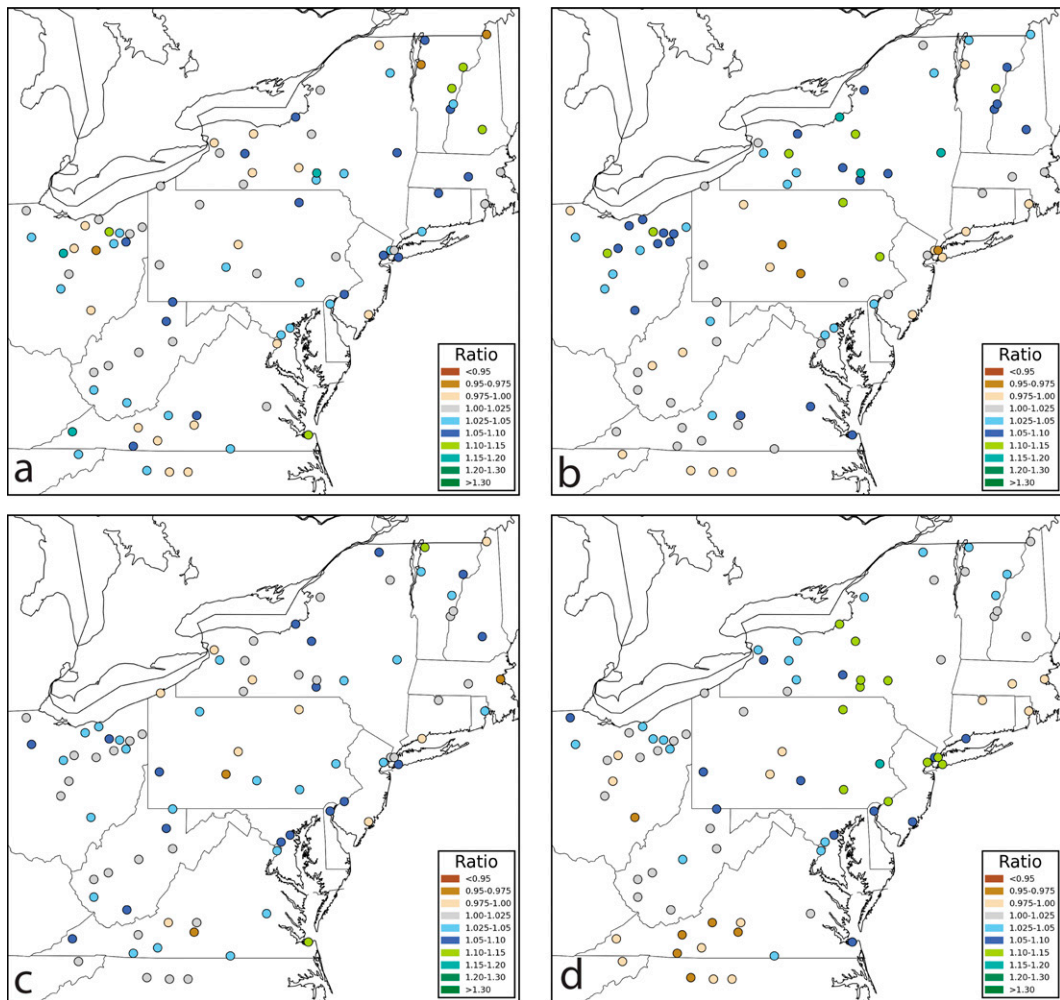


FIG. 6. As in Fig. 5, but for (a) 1-h 2-yr, (b) 1-h 100-yr, (c) 24-h 2-yr, and (d) 24-h 100-yr ARI rainfall amounts.

whereas at Schenley Lock 5 the occurrence of four PDS events exceeding the pre-2000 maximum leads to a steady increase in 100-yr ARI precipitation.

The use of 2000 as the standard base year when computing  $\Delta P_{\text{end}}$  was a practical consideration given this is the ending date for data included in *Atlas 14, volume 2*; however, it provides little insight as to how extreme rainfall in the region has evolved relative to other data periods. Figures 7 and 8 imply that if the data record ended in 1990, which is the case for other earlier extreme rainfall atlases encompassing the region (e.g., Wilks and Cember 1993), the values of  $\Delta P_{2019}$  would in some, but not all, cases exceed the values that use 2000 as the base year. Whereas, if *Atlas 14, volume 2*, had been updated in 2010, the resulting  $\Delta P_{2019}$  values would have been considerably smaller than their counterparts using base = 2000.

Figure 9 shows this to be the case across the region. There is a steady decrease in  $\Delta P_{2019}$  with base year for both the 2-yr and 100-yr RI. At more than 75% of the stations,  $\Delta P_{2019}$  exceeds 1.0 for base years from 1990 through 2000. Even for

PDS series having base years as late as 2005 and 2010, more than one-half of the stations have  $\Delta P_{2019}$  values exceeding 1.0. In general, as each additional 5-yr period is included in the base PDS, the 2-yr ARI  $\Delta P_{2019}$  value decreases by approximately 0.75% (i.e., a total change in  $\Delta P_{2019}$  of 4% between the 1990 and 2015 base year values). A similar, albeit slightly larger, change is evident for 100-yr ARI precipitation, with the  $\Delta P_{2019}$  medians for 1990 and 1995 base years nearly 5% higher than that using 2015 as the base. The  $\Delta P_{2019}$  medians also decrease more quickly, with relatively large 2% decreases associated with the 2000 and 2005 base years and little difference between  $\Delta P_{2019}$  medians for base years after 2010. Also, the  $\Delta P_{2019}$  values for the 100-yr RI are more variable among the stations than those for 2-yr RI. This is especially evident for shorter base record lengths (i.e., base years of 1990–2000).

Collectively, Fig. 9 offers some insight as to the appropriate frequency for routinely updating extreme rainfall atlases, particularly in light of recent trends in extreme rainfall and the complications that arise from the assumption of a stationary

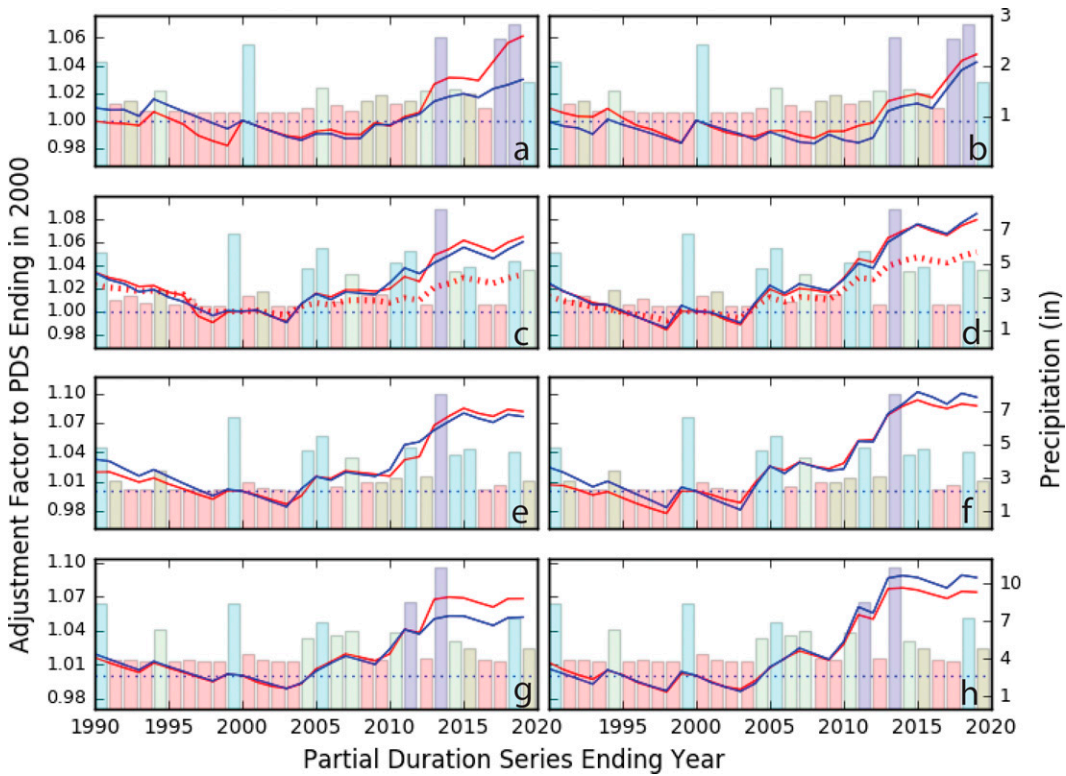


FIG. 7. The  $\Delta P_{\text{end}}$  for (a),(b) 1-h, (c),(d) 24-h, (e),(f) 1-day, and (g),(h) 7-day (left) 2- and (right) 100-yr recurrence interval rainfall amounts based on PDS ending in the specified years [the value of end in Eq. (1)] based on data for Philadelphia. The red line is the ARI amounts based on the regional L-moments analysis, and the blue line represents the L-moments fit to only the Philadelphia data. The dotted red line in (c) and (d) shows the ARI amounts based on the full 1900–2019 period of record. The bars show the largest new rainfall amount that is added to the PDS each year. Purple bars indicate that the new value is the maximum in the PDS, and light-blue, green, and brown bars indicate new values >90th percentile, between the 75th and 90th percentile, and between the 50th and 75th percentile of the PDS, respectively. Red bars are values falling below the median.

climate record in these analyses. However, other practical considerations such as the consequences of changes of this magnitude to engineering design, resilience and cost also apply. Excluding these nonclimatological factors, the statistical significance of these changes can provide some guidance as to the appropriate update interval. In the simplest case, the magnitude of the  $\Delta P_{2019}$  (using 2000 as the base) falls within the Atlas 14 90% confidence interval at nearly all stations. For those stations in the southern part of the regions (i.e., those included in Atlas 14, volume 2), the confidence intervals for both the 2- and 100-yr ARI are on the order of  $\pm 10\%$ , whereas New York and New England stations have wider  $\pm 20\%$  confidence intervals for these ARI. Thus, it could be argued that the published uncertainty bounds encompass these time-dependent variations. Nonetheless, rarely are the confidence intervals applied in practice, highlighting the need to assure that the published recurrence interval rainfall values are a true reflection of current climate conditions.

In Fig. 10, the significance of  $\Delta P_{2019}$  using 1990, 2000, and 2010 as the base is assessed at each station relative the change that would result when 30, 20, or 10 years are randomly excluded from the 70 value (1950–2019) PDS. The method in

which the PDS of all regional stations are randomized is used. Across the region the number of significant (probability  $p > 0.90$ ) positive changes increases as more years are excluded. For the 2-yr ARI, only 2% of the series show a significant positive change ( $p > 0.99$ ) using the full 70-yr PDS versus the shorter 60-yr record as compared with 6% of the series when the shorter PDS simulates a 50-yr record and 9% of series when the PDS is limited to a 40-yr record. For the 100-yr ARI, omitting the last 10 years from the simulated PDS results in a significant positive change ( $p > 0.99$ ) in 3% of the cases, whereas when the last 20 and 30 years are excluded, the change is significant in 12% and 11% of the cases, respectively. When a lower ( $p > 0.90$ ) significance level is considered, over 40% of the 50-yr time series (and 36% of the 40-yr series) show a significant change in the 100-yr ARI relative to the full 70-yr record as compared with only 27% of the 60-yr time series.

The difference between the longer and shorter PDS is more pronounced when the number of significant decreases is compared with the increases. For the 2-yr ARI, there are 4 times as many significant ( $p > 0.95$ ) increases as decreases when the last 10 years are excluded, but this proportion increases to

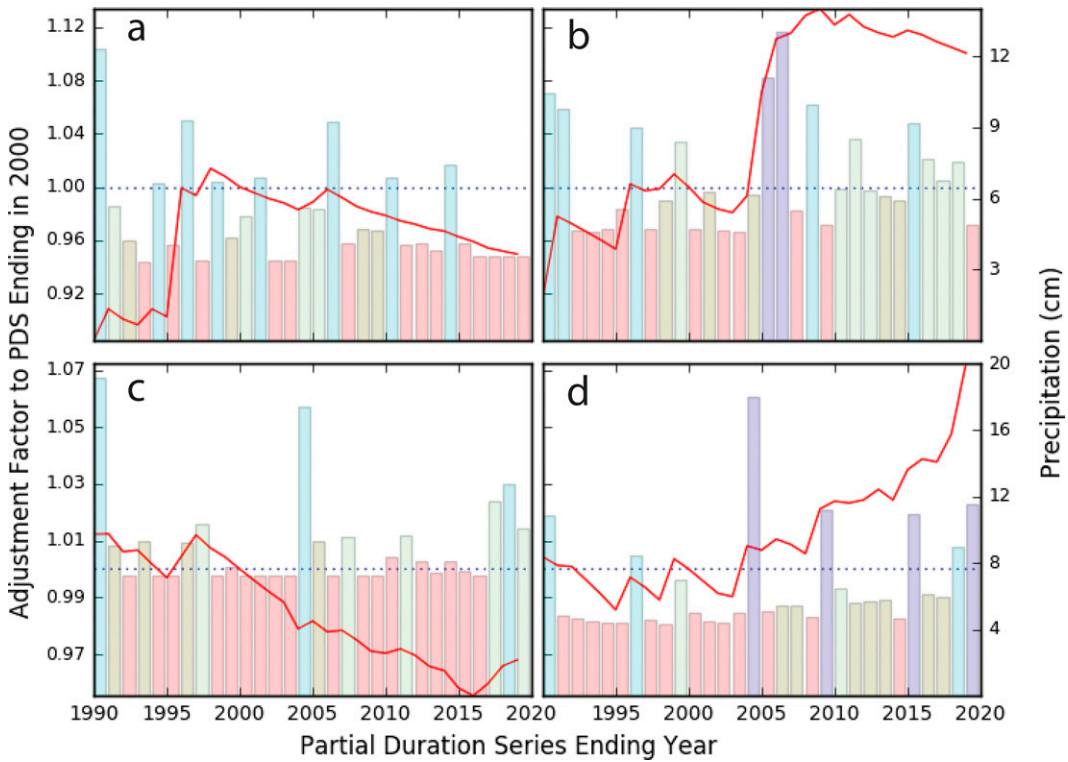


FIG. 8. The  $\Delta P_{\text{end}}$  for 1-day ARI rainfall amounts based on PDS ending in the specified years [the value of end in Eq. (1)] based on 2-yr ARI data for (a) Middleton and (b) Concord and 100-yr ARI data for (c) Indiana 3 SE and (d) Schenley Lock 5. The red line and bars are as in Fig. 7.

approximately 40–100 times as many increases as decreases when the last 20 and 30 years are excluded (Figs. 10a,c,e). For the 100-yr ARI, there are about 4 times as many significant decreases as increases based on the simulated 1950–2009 PDS as compared with over 9 times as many increases as decreases using the simulated 1950–90 PDS.

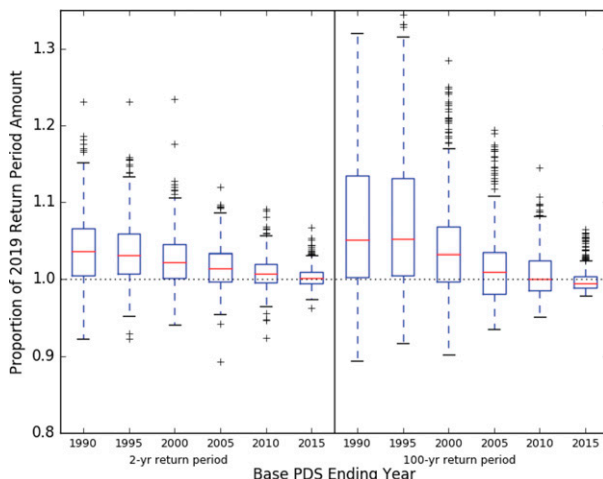


FIG. 9. Values of  $\Delta P_{2019}$  using different base years for (left) 2- and (right) 100-yr ARI precipitation amounts across all stations in the study domain.

The choice of randomization method had little effect on the results. When the base series PDS was randomized and the higher-order moments from the original regional average retained, there were more significant increase than decreases and an increase in the number of significant differences as more years were excluded from the analysis (Fig. S3 in the online supplemental material). Unlike when both the base and regional PDS were randomized the number of significant increases for the 2-yr and 100-yr ARI were similar. When the GEV distribution was fit only to randomized PDS from the base station, many more significant increases occurred for the 2-yr ARI than for the other resampling schemes, especially when the 1950–90 and 1950–2000 data records were simulated (Fig. S4 in the online supplemental material). However, very few stations showed significant changes for the 100-yr ARI (Fig. S4). This was the result of the very wide confidence intervals that resulted when the higher-order moments did not reflect a more stable regional average.

Similarly, the results for other durations were consistent with the 1-day patterns of significant differences. In Fig. S5 of the online supplemental material, the randomized regional approach is applied to 7-day precipitation duration PDS and, like the daily durations, this yielded more significant increases than decreases, more significant increases for the 2-yr ARI than for the 100-yr ARI, and an increase in the number of significant differences as more years were excluded from the analysis.

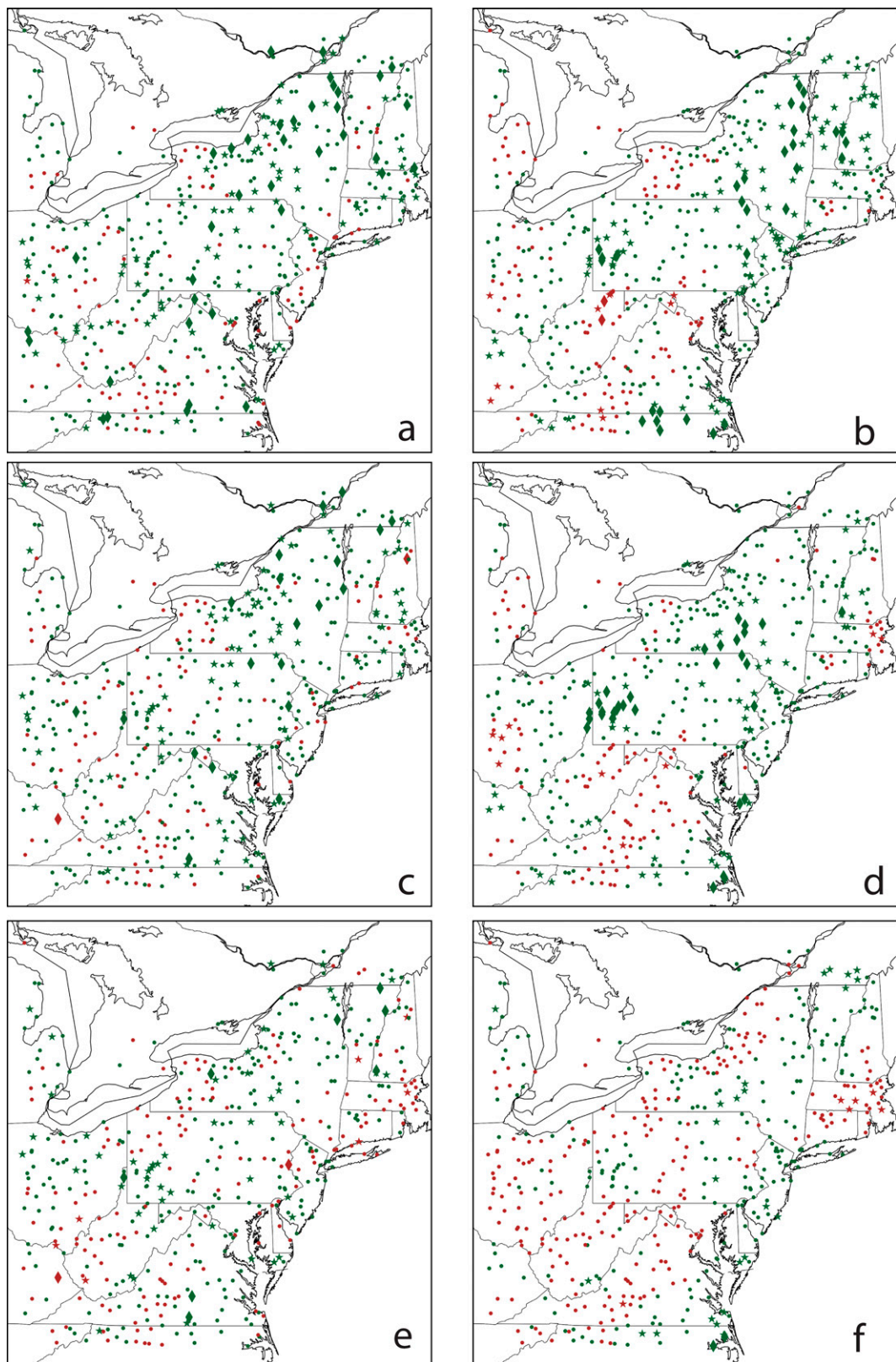


FIG. 10. Sign (color) and statistical significance (shape) of  $\Delta P_{2019}$  for daily precipitation using (a),(b) 1990, (c),(d) 2000, and (e),(f) 2010 as base years for (left) 2-yr ARI and (right) 100-yr precipitation amounts using the randomized regional PDS approach. Green symbols denote increases, and brown symbols decreases. Diamonds and stars indicate significance at the  $\alpha = 0.99$  and  $0.95$  levels, respectively.

## 5. Conclusions

Across the mid-Atlantic region of the United States, most stations with >70-yr-long daily precipitation records have seen an increase in 2-, 5-, 10-, 25-, 50-, and 100-yr recurrence interval rainfall since 2000. The positive changes occur at over 75% of the stations, with changes exceeding 2.5% at more than one-half of the stations. These changes are consistent for all ARIs and also for durations ranging from 1 to 20 days. Similar changes are also noted for hourly data, with over 75% of the observation sites experiencing increases, and 50% of these increases exceeding 2.5%. These hourly changes closely match the changes noted for daily data, indicating that when considering the most extreme events, recent increases in extreme precipitation are similar across a wide range of durations from hourly to multiday. Given that over 50% of the most extreme hourly rainfall events occur in conjunction with an extreme daily rainfall, this similarly is not surprising. As similar changes occur with rainfall durations as long as 20 days, which have much less overlap with hourly extremes, this may suggest that the mechanisms responsible for increases in the largest precipitation events may be independent of duration.

Across the region, there is not a strong spatial pattern in the observed changes in these recurrence interval rainfall amounts. Rather the increases and decreases are scattered throughout the study domain. In some locations, however, clusters or stations with predominant increases or decreases exist. This is likely an artifact of the spatial extent of specific rainfall events. Changes in the extreme ARI rainfall are strongly affected by the occurrence of one or more events in the recent record that exceed the previous maximum rainfall within the partial-duration series. Such events are likely to affect several adjacent stations leading to this clustering. Similarly neighboring stations that experienced the highest PDS events in the earlier part of their records, with few high PDS values in recent years, experience a consistent decrease in  $\Delta P_{2019}$ . This highlights that it is the occurrence of new rainfall events exceeding the previous PDS maximum or multiple new events in the upper decile of the PDS that apparently drive the observed changes in  $\Delta P_{2019}$ , rather than simply an increase in rainfall events of >99th percentile [e.g., like those used in [Groisman et al. \(2005\)](#)] that are likely to fall below the median PDS value.

Collectively, the results give some insight into the appropriate frequency at which to update extreme rainfall atlases such as NOAA Atlas 14, particularly in regions where changes in extreme rainfall frequency are evident. Decadal updates, as is common with climate normals ([Arguez et al. 2012](#)), are not warranted as the number of significant changes is small, the proportion of positive and negative changes are relatively similar, and the magnitude of most changes is within  $\pm 2.5\%$  of the full-record value. Routine updates on a cycle from 20 to at most 30 years, however, should be considered. Over this interval, many more stations show significant changes. Increases in extreme rainfall have been experienced at over 75% of the stations during these time intervals, with the magnitude of change for the longest ARIs exceeding 10% at

one-quarter of the long-term stations in the region. Changes of this magnitude generally exceed the current Atlas 14 confidence bounds in those states covered by NOAA Atlas 14, volume 2.

Although these results provide some guidance as to the rational update frequency for extreme rainfall analyses, an additional consideration that is beyond the scope of this work, is the extent to which the earliest years should be considered at stations with long periods of record like Philadelphia ([Fig. 7c](#)). In such cases, where few PDS members exist in the early part of the record, including the entire record (i.e., not excluding the earliest years) tempers the magnitude of change that results from any increase in the frequency of extreme events in recent years. A 70-yr record was adopted here, in line with [DeGaetano and Castellano \(2018\)](#) who showed that the influence of modestly nonstationary PDS tended to be minimized for this record length. Adopting a fixed limit on PDS length in practice, however, is not ideal because it could potentially exclude large PDS that occurred earlier in the record. A potential approach would be to test longer-than-70-yr PDS for significant trends in the location parameter of the fit distribution and choose PDS on the basis of these results. This approach would be particularly relevant in regions where precipitation extremes exhibit patterns of interdecadal variability.

**Acknowledgments.** This work was supported by the State of New Jersey via AECOM Project 60629640; partial support from NOAA Contract 1332KP21FNEEN0023 is also acknowledged. We are grateful for technical and scientific support from Drs. David Robinson and Nick Procopio.

**Data availability statement.** The data used in this work can be obtained from the NOAA National Centers for Environmental Information. Daily data are a part of the Global Historical Climatology Network Daily (GHCN-D) dataset. Hourly data were extracted from COOP-Hourly Precipitation Data (HPD), version 2; NCEI Hourly Precipitation Dataset (HPD; DSI-3240); and NCEI Surface Data Hourly Global (DS3505). Analysis software, as cited in the work, is open source and is accessible online (<https://www.scipy.org> and [pypi.org](https://pypi.org)).

## REFERENCES

Arguez, A., I. Durre, S. Applequist, R. S. Vose, M. F. Squires, X. Yin, R. R. Heim Jr., and T. W. Owen, 2012: NOAA's 1981–2010 U.S. Climate Normals: An overview. *Bull. Amer. Meteor. Soc.*, **93**, 1687–1697, <https://doi.org/10.1175/BAMS-D-11-00197.1>.

Armstrong, W. H., M. J. Collins, and N. P. Snyder, 2014: Hydro-climatic flood trends in the Northeastern United States and linkages with large-scale atmospheric circulation patterns. *Hydrol. Sci. J.*, **59**, 1636–1655, <https://doi.org/10.1080/02626667.2013.862339>.

Bonnin, G. M., D. Martin, B. Lin, T. Parzybok, M. Yekta, and D. Riley, 2006: Delaware, District of Columbia, Illinois, Indiana, Kentucky, Maryland, New Jersey, North Carolina, Ohio, Pennsylvania, South Carolina, Tennessee, Virginia, West

Virginia. Precipitation-Frequency Atlas of the United States, vol. 2, version 3.0, NOAA Atlas 14, 295 pp., [https://www.weather.gov/media/owp/oh/hdsc/docs/Atlas14\\_Volume2.pdf](https://www.weather.gov/media/owp/oh/hdsc/docs/Atlas14_Volume2.pdf).

Brown, V. M., B. D. Keim, and A. W. Black, 2020: Trend analysis of multiple extreme hourly precipitation time series in the southeast United States. *J. Appl. Meteor. Climatol.*, **59**, 427–442, <https://doi.org/10.1175/JAMC-D-19-0119.1>.

Cheng, L., and A. AghaKouchak, 2014a: Nonstationary precipitation intensity-duration-frequency curves for infrastructure design in a changing climate. *Sci. Rep.*, **4**, 7093, <https://doi.org/10.1038/srep07093>.

—, —, E. Gilleland, and R. W. Katz, 2014b: Non-stationary extreme value analysis in a changing climate. *Climatic Change*, **127**, 353–369, <https://doi.org/10.1007/s10584-014-1254-5>.

Collins, M. J., 2009: Evidence for changing flood risk in New England since the late 20th century. *J. Amer. Water Resour. Assoc.*, **45**, 279–290, <https://doi.org/10.1111/j.1752-1688.2008.00277.x>.

Cooley, A., and H. Chang, 2017: Precipitation intensity trend detection using hourly and daily observations in Portland, Oregon. *Climate*, **5**, 10, <https://doi.org/10.3390/cli5010010>.

Coumou, D., and S. Rahmstorf, 2012: A decade of weather extremes. *Nat. Climate Change*, **2**, 491–496, <https://doi.org/10.1038/nclimate1452>.

DeGaetano, A. T., 2009: Time-dependent changes in extreme-precipitation return-period amounts in the continental United States. *J. Appl. Meteor. Climatol.*, **48**, 2086–2099, <https://doi.org/10.1175/2009JAMC2179.1>.

—, and C. M. Castellano, 2017: Future projections of extreme precipitation intensity-duration-frequency curves for climate adaptation planning in New York State. *Climate Serv.*, **5**, 23–35, <https://doi.org/10.1016/j.cliser.2017.03.003>.

—, and —, 2018: Selecting time series length to moderate the impact of non-stationarity in extreme rainfall analyses. *J. Appl. Meteor. Climatol.*, **57**, 2285–2296, <https://doi.org/10.1175/JAMC-D-18-0097.1>.

Donat, M. G., A. L. Lowry, L. V. Alexander, P. A. O’Gorman, and N. Maher, 2016: More extreme precipitation in the world’s dry and wet regions. *Nat. Climate Change*, **6**, 508–513, <https://doi.org/10.1038/nclimate2941>.

Fischer, E. M., and R. Knutti, 2016: Observed heavy precipitation increase confirms theory and early models. *Nat. Climate Change*, **6**, 986–991, <https://doi.org/10.1038/nclimate3110>.

Georgakakos, A., P. Fleming, M. Dettinger, C. Peters-Lidard, T. C. Richmond, K. Reckhow, K. White, and D. Yates, 2014: Water resources. Climate change impacts in the United States: The Third National Climate Assessment, J. M. Melillo, T. C. Richmond, and G. W. Yohe, Eds., U.S. Global Change Research Program Rep., 69–112, <https://doi.org/10.7930/J0G44N6T>.

Groisman, P. Ya., 1992: Studying the North American precipitation changes during the last 100 years. *Proc. Fifth Int. Meeting on Statistical Climatology*, Toronto, ON, Canada, Amer. Meteor. Soc., 75–79.

—, R. W. Knight, D. R. Easterling, T. R. Karl, G. C. Hegerl, and V. N. Razuvavaev, 2005: Trends in intense precipitation in the climate record. *J. Climate*, **18**, 1326–1350, <https://doi.org/10.1175/JCLI3339.1>.

—, —, and T. R. Karl, 2012: Changes in intense precipitation over the central United States. *J. Hydrometeor.*, **13**, 47–66, <https://doi.org/10.1175/JHM-D-11-039.1>.

Heineman, M., 2012: Trends in precipitation maxima at U.S. Historical Climatology Network Stations: 1893–2010. *Proc. World Environmental and Water Resources Congress 2012: Crossing Boundaries*, American Society of Civil Engineers, 2003–2012, <https://doi.org/10.1061/9780784412312.201>.

Hosking, J. R., 1990: L-moments: Analysis and estimation of distributions using linear combinations of order statistics. *J. Roy. Stat. Soc.*, **52B**, 105–124, <https://doi.org/10.1111/j.2517-6161.1990.tb01775.x>.

Katz, R., 2010: Statistics of extremes in climate change. *Climatic Change*, **100**, 71–76, <https://doi.org/10.1007/s10584-010-9834-5>.

Kenyon, J., and G. C. Hegerl, 2010: Influence of modes of climate variability on global precipitation extremes. *J. Climate*, **23**, 6248–6262, <https://doi.org/10.1175/2010JCLI3617.1>.

Kunkel, K. E., 2003: North American trends in extreme precipitation. *Nat. Hazards*, **29**, 291–305, <https://doi.org/10.1023/A:1023694115864>.

—, K. Andsager, and D. R. Easterling, 1999: Long-term trends in extreme precipitation events over the conterminous United States and Canada. *J. Climate*, **12**, 2515–2527, [https://doi.org/10.1175/1520-0442\(1999\)012<2515:LTTIEP>2.0.CO;2](https://doi.org/10.1175/1520-0442(1999)012<2515:LTTIEP>2.0.CO;2).

—, and Coauthors, 2013: Climate of the Northeast U.S. Part 1, Regional Climate Trends and Scenarios for the U.S. National Climate Assessment, NOAA Tech. Rep. NESDIS 142-1, 80 pp., [https://scenarios.globalchange.gov/sites/default/files/NOAA\\_NESDIS\\_Tech\\_Report\\_142-1-Climate\\_of\\_the\\_Northeast\\_U.S.\\_1.pdf](https://scenarios.globalchange.gov/sites/default/files/NOAA_NESDIS_Tech_Report_142-1-Climate_of_the_Northeast_U.S._1.pdf).

Lau, K. M., Y. P. Zhou, and H. T. Wu, 2008: Have tropical cyclones been feeding more extreme rainfall? *J. Geophys. Res.*, **113**, D23113, <https://doi.org/10.1029/2008JD009963>.

Lenderink, G., H. Y. Mok, T. C. Lee, and G. J. Van Oldenborgh, 2011: Scaling and trends of hourly precipitation extremes in two different climate zones—Hong Kong and the Netherlands. *Hydrol. Earth Syst. Sci.*, **15**, 3033–3041, <https://doi.org/10.5194/hess-15-3033-2011>.

Menne, M. J., I. Durre, R. S. Vose, B. E. Gleason, and T. G. Houston, 2012: An overview of the Global Historical Climatology Network-Daily database. *J. Atmos. Oceanic Technol.*, **29**, 897–910, <https://doi.org/10.1175/JTECH-D-11-00103.1>.

Myhre, G., and Coauthors, 2019: Frequency of extreme precipitation increases extensively with event rareness under global warming. *Sci. Rep.*, **9**, 16063, <https://doi.org/10.1038/s41598-019-52277-4>.

Ning, L., E. E. Riddle, and R. S. Bradley, 2015: Projected changes in climate extremes over the northeastern United States. *J. Climate*, **28**, 3289–3310, <https://doi.org/10.1175/JCLI-D-14-00150.1>.

Papalexiou, S. M., and D. Koutsoyiannis, 2013: Battle of extreme value distributions: A global survey on extreme daily rainfall. *Water Resour. Res.*, **49**, 187–201, <https://doi.org/10.1029/2012WR012557>.

Perica, S., S. Pavlovic, M. St. Laurent, C. Trypaluk, D. Unruh, D. Martin, and O. Wilhite, 2019: Northeastern states: Connecticut, Maine, Massachusetts, New Hampshire, New York, Rhode Island, Vermont. Precipitation-Frequency Atlas of the United States, vol. 10, version 3.0, NOAA Atlas 14, 265 pp., [https://www.weather.gov/media/owp/hdsc\\_documents/Atlas14\\_Volume10.pdf](https://www.weather.gov/media/owp/hdsc_documents/Atlas14_Volume10.pdf).

Peterson, T. C., and Coauthors, 2013: Monitoring and understanding changes in heat waves, cold waves, floods, and droughts in the United States: State of knowledge. *Bull. Amer. Meteor. Soc.*, **94**, 821–834, <https://doi.org/10.1175/BAMS-D-12-00066.1>.

Prein, A. F., and L. O. Mearns, 2021: U.S. extreme precipitation weather types increased in frequency during the 20th century.

*J. Geophys. Res. Atmos.*, **126**, e2020JD034287, <https://doi.org/10.1029/2020JD034287>.

Shepherd, J. M., A. Grundstein, and T. L. Mote, 2007: Quantifying the contribution of tropical cyclones to extreme rainfall along the coastal southeastern United States. *Geophys. Res. Lett.*, **34**, L23810, <https://doi.org/10.1029/2007GL031694>.

Sun, Q., C. Miao, and Q. Duan, 2016: Extreme climate events and agricultural climate indices in China: CMIP5 model evaluation and projections. *Int. J. Climatol.*, **36**, 43–61, <https://doi.org/10.1002/joc.4328>.

Walsh, J., and Coauthors, 2014: Our changing climate. Climate change impacts in the United States: The Third National Climate Assessment, J. M. Melillo, T. C. Richmond, and G. W. Yohe, Eds., U.S. Global Change Research Program Rep., 19–67, <https://doi.org/10.7930/J0KW5CXT>.

Wilks, D. S., and R. P. Cember, 1993: Atlas of precipitation extremes for the northeastern United States and southeastern Canada. Northeast Regional Climate Center Publ. RR 93-5, 40 pp.

Wuertz, D., J. Lawrimore, and B. Korzeniewski, 2018: Cooperative Observer Program (COOP) Hourly Precipitation Data (HPD), version 2.0. NOAA National Centers for Environmental Information, accessed 19 May 2020, <https://doi.org/10.25921/p7j8-2170>.

Yarnell, D. L., 1935: Rainfall intensity-frequency data. U.S. Department of Agriculture Miscellaneous Publ. S04, 68 pp.

Yu, L., S. Zhong, L. Pei, X. Bian, and W. E. Heilman, 2016: Contribution of large-scale circulation anomalies to changes in extreme precipitation frequency in the United States. *Environ. Res. Lett.*, **11**, 044003, <https://doi.org/10.1088/1748-9326/11/4/044003>.